

P. Verheyden  
S. Katscher  
Th. Schulz  
F. Schmidt  
Ch. Josten

## Open MR imaging in spine surgery: experimental investigations and first clinical experiences

Received: 30 July 1999  
Accepted: 7 August 1999

**Abstract** *Introduction:* The latest open MRI technology allows to perform open and closed surgical procedures under real-time imaging. Before performing spinal trauma surgery preclinical examinations had to be done to evaluate the artifacts caused by the implants. *Methods:* The MRT presented is a prototype developed by GE. Two vertically positioned magnetic coils are installed in an operation theater. By that means two surgeons are able to access the patient between the two coils. Numerous tests regarding the material of instruments and implants were necessary in advance. The specific size of the artifact depending on the pulse sequence and the positioning within the magnetic field had to be examined. *Results:* The magnifying factors of the artifact in the spin echo sequence regarding titanium are between 1.7 and 3.2, depending on the direction of the magnetic vector. Regarding stainless steel they are between 8.4 and 8.5. In the gradient echo sequence the factors are between 7.5 and 7.7 for titanium and between 16.9 and 18.0 for stainless steel. The tip of an implant is imaged with an accuracy of 0 to 2 mm. Since September 1997 16 patients

with unstable fractures of the thoracic and lumbar spine have been treated by dorsal instrumentation in the open MRI. Percutaneous insertion of the internal fixator has proven a successful minimally invasive procedure. The positioning of the screws in the pedicle is secure, the degree of indirect reduction of the posterior wall of the vertebral body can be imaged immediately. The diameter of the spinal canal can be determined in any plane. *Discussion and conclusion:* The open MRI has proven useful in orthopedic and trauma surgery. The size and configuration of the artifacts caused by instruments and implants is predictable. Therefore exact positioning of the implants is achieved more easily. Dorsal instrumentation of unstable thoracolumbar fractures with a percutaneous technique has turned out safe and less traumatic under MR-imaging. Real-time imaging of soft tissue and bone in any plane improves security for the patient and allows the surgeon to work less invasively and more precisely.

**Key words** Open MRI · Spinal fractures · Internal fixator · Percutaneous · Artifacts

P. Verheyden (✉) · S. Katscher  
Ch. Josten  
Department of Traumatology,  
University of Leipzig, Liebigstrasse 20a,  
D-04103 Leipzig, Germany  
e-mail: verhey@medizin.uni-leipzig.de,  
Tel.: +49-341-971 7322  
Fax: +49-341-971 7319

Th. Schulz · F. Schmidt  
Department of Radiology,  
University of Leipzig, Leipzig, Germany

### Introduction

The standard treatment for unstable thoracolumbar spine fractures, especially in Europe, is the dorsal instrumenta-

tion with the fixateur interne [5]. Restoration of vertebral body height and realignment of the spine by certain repositioning techniques can be viewed by fluoroscopy. However, there are problems in imaging the position of the posterior wall fragment. Intraoperative myelography or sonog-

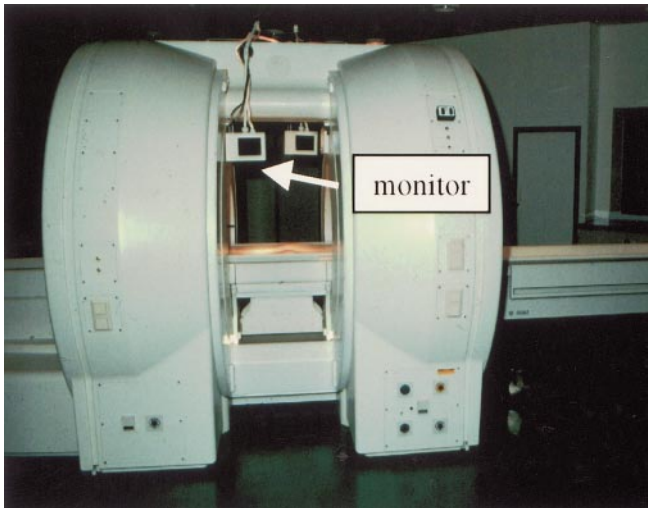


**Fig. 1** Open MRT

raphy through a small hemilaminectomy, which requires a surgeon with particular expertise, can be used as supplementary imaging methods [3]. If there is an obstruction of the spinal canal followed by neurological deficit, more invasive steps with a destabilizing laminectomy become necessary [4]. Otherwise the risk of spinal cord compression remains [1].

The methods described above are not feasible for less invasive percutaneous implantation of the internal fixator with indirect reduction.

The open Magnetic Resonance Tomograph (Signa SP, GEMS, USA), which is installed in an aseptic operating theatre (Fig. 1), provides a new method for intraoperative visualization of anatomical structures. Two vertically positioned magnetic coils produce a homogeneous 0.5-T magnetic field ( $B_0$  field) in between. The region of interest of the patient has to be placed between the coils, and two surgeons are then able to perform open and closed procedures under real-time imaging in any plane.

To develop a safe and less invasive surgical method for unstable spine fractures under open MRI conditions, it was first necessary to evaluate whether MR imaging is reliable for intraoperative monitoring. The only references to this in the literature relate to experiences regarding biopsy needles [12]. It was therefore necessary to investigate how much artifacts caused by instruments and implants disturb the quality of imaging. It is vital to know exactly where in the surrounding artifact the instrument is located. The artifact has to be predictable.

### Scientific background

MRI is based on stimulation of hydrogen protons, which are lined up in the magnetic field because of their polarity. Stimulation is created by electromagnetic impulses with

**Table 1** Determinants of artifacts in open MRI

Material-specific characteristics
Susceptibility
Diameter of the material
Material-independent characteristics
Equipment-specific factors (coils, magnetic field strength)
Technique of imaging (spin echo or gradient echo sequences)
Movement (breathing)

defined parameters. The total magnetizing vector changes its direction depending on the strength and duration of the impulse. In the idealized three-dimensional model at that time ( $T_0$ ), all the hydrogen protons are orientated in the  $xy$ -plane and point in the same direction.

The hydrogen protons return most (63.21%) of the absorbed energy as electromagnetic waves (resonance) in a short time ( $T_1$ ). The resulting resonance signals can be received and transformed in the  $T_1$ -weighted image. A second MRI-specific phenomenon is the divergence of the vectors by interactions between the protons. The computer transforms the resulting signals to the  $T_2$ -weighted image.

An image consists of small three-dimensional elements, called voxels. The quality of imaging increases with smaller voxels. But the size of the voxels is limited by the intensity of their signals [11].

In MR imaging, not only a similar impulse but sequences of impulses are used. The duration from the beginning of one sequence of impulses to the next one is called repetition time (TR).

Spin echo sequences (SE) and gradient echo sequences (GE) are the most common techniques. SE is characterized by an initial  $90^\circ$  impulse followed by  $180^\circ$  impulses after a certain time. The advantage of SE is a brilliant picture, but it requires repetition times (TR) of some seconds, and so it needs several minutes for the image. Consequences are delayed information and artifacts caused by movement. GE sequences provide faster information under operating conditions. Much shorter TRs allow faster imaging, in 3–5 s. The disadvantage of this technique is the sensibility to changes of the magnetic field and differences in the susceptibility of different materials. The susceptibility is a measure of the magnetizability of a material – tissue or implant. The bigger the differences in susceptibility between different materials is, the bigger an extinguishing phenomenon in the image appears, which means a loss of information. The area defined by extinguishing phenomena, where anatomical structures are not clear, we call artifact (Table 1).

### Preclinical investigations in open MR imaging

Recent literature about artifacts by instruments and implants on MR images focuses on techniques to minimize the artifact [6, 9, 17]. To perform less invasive spine sur-

gery under real-time control with open MRI, it is essential to know exactly where the instrument or implant is located in the artifact. Only a few investigations concerning biopsy needles have been published [9, 12].

Other studies about artifacts after instrumentation of the spine focus on the question how the imaging of the spinal canal is disturbed [16].

## Methods

Titanium and stainless steel, which are mainly used for instruments and implants, were fixed in gelatin of a defined composition (87.5% H<sub>2</sub>O and 12.5% gelatin or 25% H<sub>2</sub>O, 12.5% gelatin and 62.5% glycerol).

Wires with a diameter of 1.6 mm were compared to establish the material-specific artifacts. To examine the material-independent factors, exclusively 1.6-mm titanium wires were used. The influence of the surrounding conditions was tested by adding glycerol to the gelatin. Sagittal, transversal and coronal planes were examined with the wires placed vertically to the B0 field.

Different sequences (SE and GE), different directions of the impulse, T1- and T2-weighted images with corresponding repetition times (TR) were examined in all planes. For comparison, a plexiglas pin was used, which has a susceptibility equal to gelatin and therefore causes no artifact. The analysis was done with the central computer using a 512 matrix.

## Results

The following data present the results according to the material used (Table 2, Fig. 2) as well as the plane of imaging (Table 3, Fig. 3) for spin echo and gradient echo sequences.

It is clear that even non-ferromagnetic materials cause considerable artifacts. Steel is not useful in open MRI, because of its 2.4 (GE) to 4.8 (SE) times higher extinction

**Table 2** Comparison of measurements (in mm) and magnifying factors (MF)<sup>a</sup> of steel and titanium wires (vertical to B0 field) with diameter of 1.6 mm (parameters: FOV 12 × 12; Matrix 512 × 128; Nex 2; St 7 mm; Is 1 mm)

	Steel		Titanium	
	Extinction	MF	Extinction	MF
<b>Spin echo</b>				
T1 (TR 440) ↑	13.4	8.4	5.2	3.2
T2 (TR 2500) ↑	13.5	8.4	5.2	3.2
T1 (TR 440) →	13.6	8.5	2.8	1.7
T2 (TR 2500) →	13.6	8.5	2.8	1.7
<b>Gradient echo</b>				
T1 (TR 60) ↑	27.1	16.9	12.4	7.7
T2 (TR 35) ↑	28.8	18.0	12.0	7.5
T1 (TR 60) →	28.0	17.5	12.4	7.7
T2 (TR 35) →	28.6	17.8	12.1	7.5

<sup>a</sup>Magnifying factor = extinction (mm) / real diameter (1.6 mm) of the wire

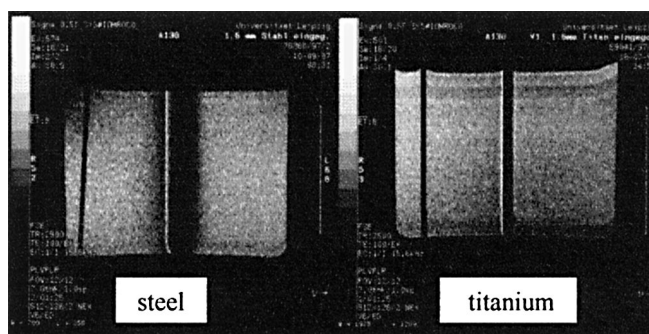


**Fig. 2** Artifacts of steel- and titanium wires (Ø 1.6 mm, perpendicular to B0-field)

compared to titanium. For titanium, the magnification factor of the real diameter is 1.7–3.2 (SE) to 7.5–7.7 (GE).

In the GE sequences, which are used for nearly real-time imaging, the magnifying factor differs by only 0.2 across various planes. Other examinations showed that the magnifying factor decreases with increasing diameter of the implant (Table 4).

Another important finding of further tests was that, independent of the diameter of the artifact, the tip of an implant or instrument is imaged to an accuracy of 2 mm (Table 5).

Concerning the nearly real-time GE sequences, there are only minimal differences caused by change of plane and change of impulse direction. The degree of extinction depends mainly on the material. So the artifact is constant and reliable for calculation.

SE sequences cause less artifacts and are useful for more exact preoperative and postoperative images as well as intraoperative control of the posterior wall fragment. The disadvantage is the longer time of imaging. The direction of impulses and the orientation of the longitudinal axis regarding the B0 field have to be included in the calculation of artifacts by a maximum difference of factor 2. The size of the artifact decreases if the longitudinal axis of the instrument or implant is orientated parallel to the B0 field. The highest accuracy in determining the tip of an implant is achieved when the longitudinal axis is positioned vertical to the B0 field.

## MRI-assisted spine surgery

All implants and instruments are made out of non-ferromagnetic materials, like titanium or titanium alloys. All equipment for anesthesiology has to be free of ferromagnetic parts and has to be shielded, so that high frequency signals do not disturb the MR images.

To perform spine surgery the patient is positioned and fixed in prone position axially within the two doughnut coils on the table. Thorax and pelvis should be supported by silicon-pads. A flexible coil is fixed on the back of the

**Table 3** Comparison of measurements (in mm) and magnifying factors by plane of imaging for the artifact of a titanium wire (vertical to the B0 field)

	Axial		Sagittal		Coronal	
	Extinction	MF	Extinction	MF	Extinction	MF
Spin echo						
T1 (TR 440) →	5.2	3.2	2.4	1.5	4.9	3.0
T2 (TR 2500) →	5.2	3.2	2.4	1.5	4.7	2.9
T1 (TR 440) ↑	2.8	1.7	5.2	3.2	4.7	2.9
T2 (TR 2500) ↑	2.8	1.7	4.9	3.0	4.7	2.9
Gradient echo						
T1 (TR 60) →	12.4	7.7	12.2	7.6	7.0	4.4
T2 (TR 35) →	12.0	7.5	11.9	7.4	7.2	4.5
T1 (TR 60) ↑	12.4	7.7	12.2	7.6	7.2	4.5
T2 (TR 35) ↑	12.1	7.5	11.9	7.4	7.3	4.6

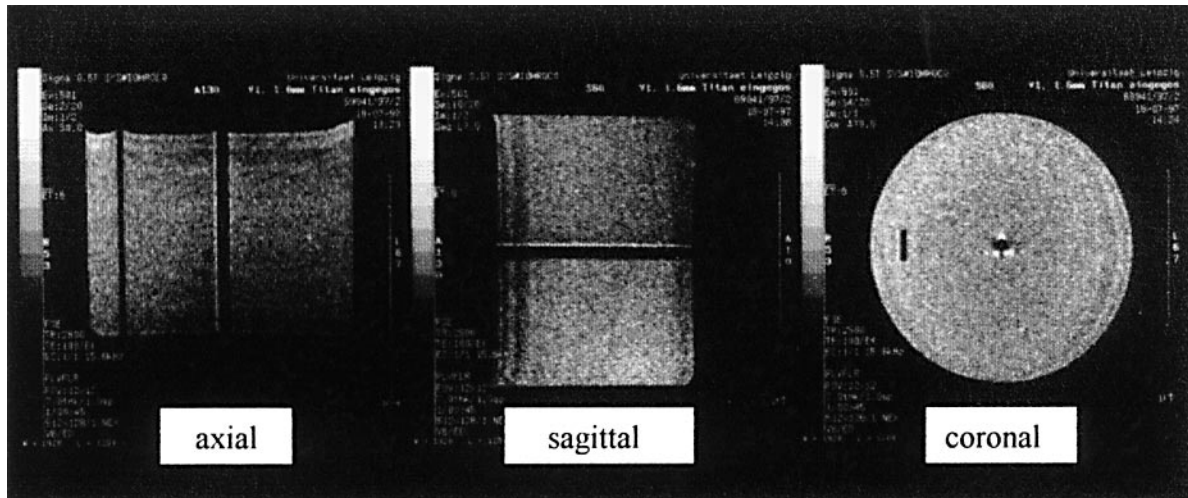


**Fig. 3** Influence of the plane of imaging (titanium wire  $\varnothing$  1.6 mm, perpendicular to B0-field)

**Table 4** Measurements (in mm) and magnifying factors of titanium pedicle screws with 6 mm diameter (vertical to the B0 field)

	Extinction	MF
Spin echo		
T1 (TR 440) →	9.4	1.6
T2 (TR 2500) →	9.1	1.5
T1 (TR 440) ↑	10.0	1.7
T2 (TR 2500) ↑	10.2	1.7
Gradient echo		
T1 (TR 60) →	25.5	4.3
T2 (TR 35) →	24.8	4.1
T1 (TR 60) ↑	26.2	4.4
T2 (TR 35) ↑	25.3	4.2

patient. The fractured vertebra should be located in the center of the flexible coil.

After positioning of the patient, the radiologist starts the first SE sequence, which lasts little more than 1 min.

**Table 5** Measured distance (in mm) of the tip of a pedicle screw with a real distance of 10 mm in the axial plane (pedicle screw vertical to the B0 field)

	Measured distance
Spin echo	
T1 (TR 440) →	10
T2 (TR 2500) →	9
T1 (TR 440) ↑	10
T2 (TR 2500) ↑	9
Gradient echo	
T1 (TR 60) →	8
T2 (TR 35) →	8
T1 (TR 60) ↑	9
T2 (TR 35) ↑	9

The surgeons can see the images in any plane on the monitor.

Two surgeons face each other across the two vertical coils and the patient. An integrated navigation system (Flashpoint Position Encoder, IGT, USA) is available for three-dimensional orientation (Fig. 4). This LED-based navigation system can be connected to several instruments. A camera above the operating field receives the signals

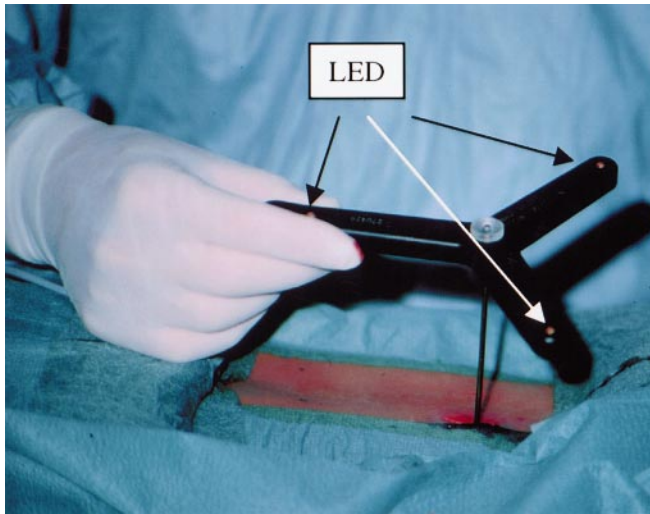


**Fig. 4** LED based navigation system

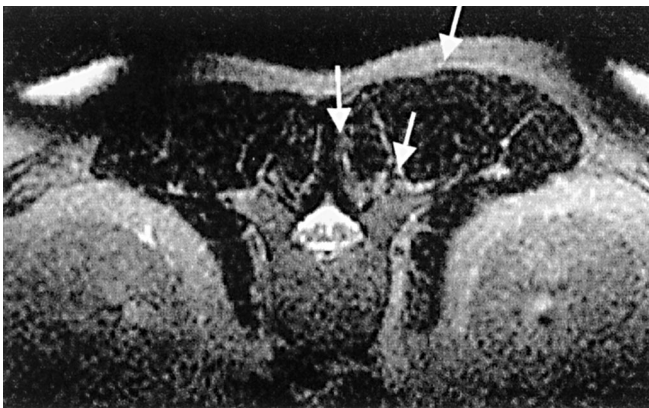


**Fig. 5** Percutaneous access (lateral – medial – lateral)

from the light-emitting diodes. The tip of a Kirschner-wire, which is connected to the Flashpoint-System, can be visualized in any plane in nearly real time. Supported by this instrument, the stab incisions are defined on the skin. The fascia is incised parallel to the skin incision more medially, besides the supraspinous ligament, and the erector trunci muscle is carefully pushed away laterally (Fig. 5), so no muscle has to be removed from the vertebrae. Supported by the navigation system, the point of entry to the pedicle can be identified in the axial and sagittal planes (Fig. 6). The pedicle is opened with an awl and the screws are inserted. All manipulations can be viewed on the monitor (Fig. 7). The position of the tip of the screw can be determined to an accuracy of 2 mm.

After insertion of all pedicle screws (Fig. 8), a gentle tunneling of the subfascial space allows the rods to be introduced and connected to the clamps and screws. When the instrumentation is completed, it is pushed down close to the lamina for biomechanical reasons, without compro-

misging the segmental muscles. Reduction is then performed in terms of lordosis and, when needed, distraction. The process of reduction can be watched in nearly real-time, and is finally documented by a spin echo sequence (Fig. 9). If the realignment of the retropulsed posterior wall fragment is insufficient, direct reduction can be achieved by a small hemilaminectomy.

Sufficient readaptation of the fascia is important to prevent secondary soft tissue problems caused by the implants.

### Clinical results

Since September 1997, 16 patients with unstable fractures of the thoracolumbar spine compromising the spinal canal through a posterior wall fragment have been treated by dorsal instrumentation under real-time control using open MRI. Instrumentation was performed with an internal fixator system (USS, Synthes, Switzerland).

A 30–50% longer time for anesthesia compared to the conventional procedure was observed due to positioning of the patient as well as for pre-, intra- and postoperative MR sequences. The blood loss from the percutaneous instrumentation was nearly zero, no suction unit is required. Remobilization was possible the 1st day after surgery in all patients.

No perioperative complications occurred. Postoperatively we had one case of temporary plexus irritation caused by positioning the arms on top of the head. Ever since that incident, the arms have been placed beside the trunk. Two cases of aseptic seroma were observed, caused by direct insertion of the pedicle through the m. erector trunci. After changing the incision of the fascia medially to the muscle, this complication didn't occur any more.

For validation of the MR imaging, the patients were re-examined by CT. Positioning of the screws was always within in pedicle. The degree of realignment of the spinal canal was comparable on CT and MRI. The location of the implants in the artifact were confirmed as corresponding with the findings of the described investigations.

### Discussion

Artifacts in MR imaging are minimized by shorter echo times (TE), lower field strengths, higher readout bandwidths (Bws) and smaller voxel sizes [16]. Changes of repetition time do not make much difference. A significant decrease in the artifact is obtained if the voxel size is minimized to 1 mm<sup>3</sup> [2, 13]. Rudisch et al. found out that T1- and proton density-weighted images with short TE evoke fewer artifacts than T2-weighted images with longer TE [17]. Wang et al. found the best imaging of the spine in the presence of pedicle screws on T1-weighted images with a TE of 16 ms and a TR of 500–600 ms; the optimal values on T2-weighted images were with a TE of 60 ms and a TR of 1300–1600 ms [18].

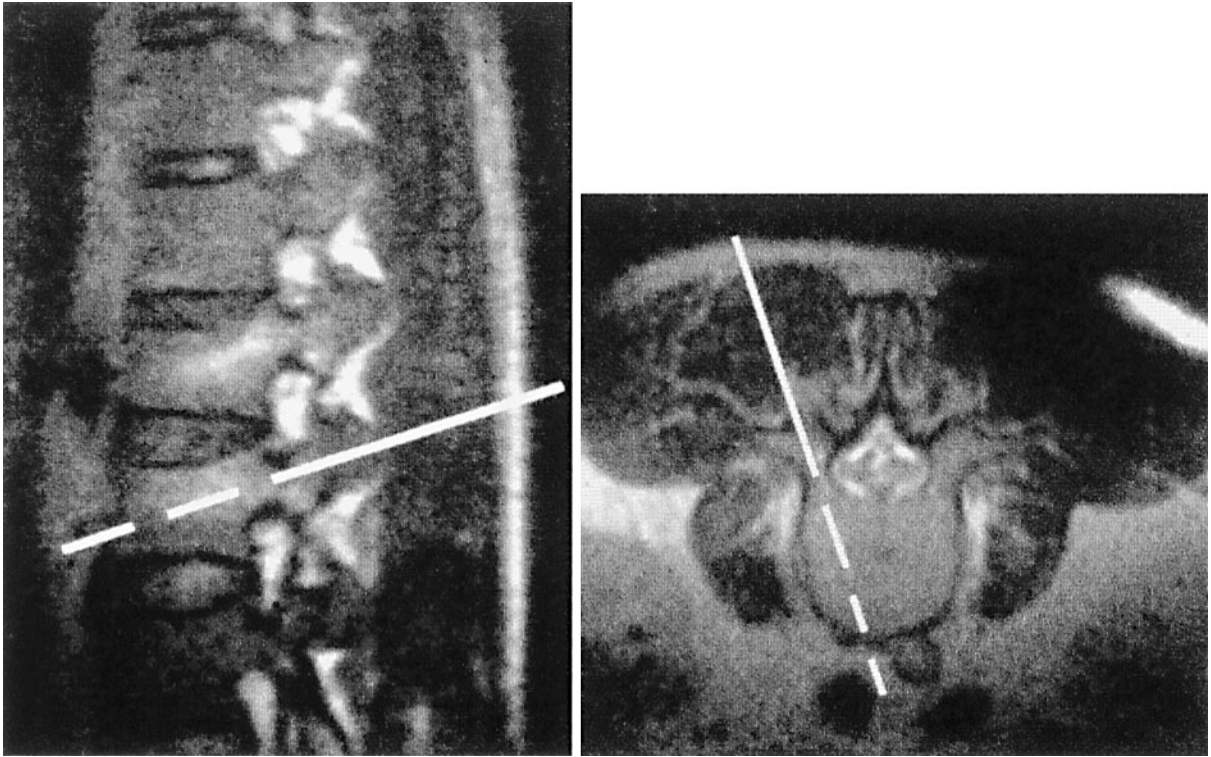


**Fig. 6** Identification of the insertion point in the pedicle

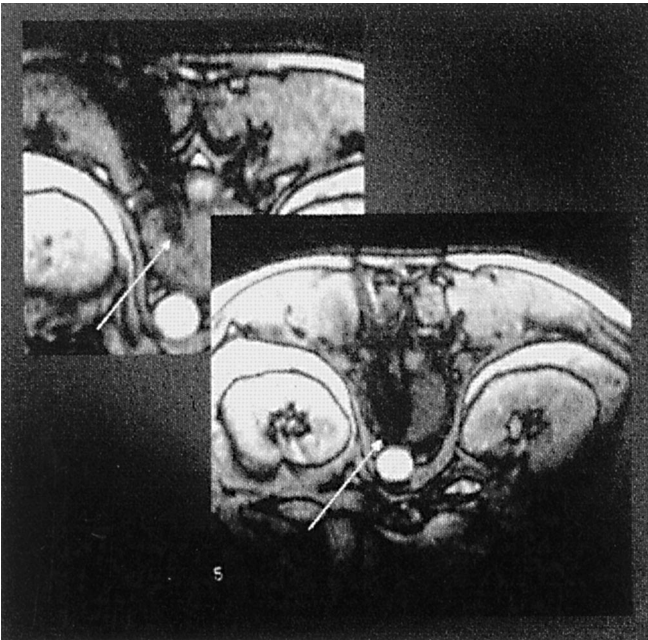


**Fig. 7** Insertion of the screw (tip can be defined with an accuracy of 2 mm)



**Fig. 8** Situs after insertion of pedicle screws

Petersilge et al. looked at the artifacts caused by pedicle screws on the axial and sagittal view. The zone of signal void surrounded by the zone of high signal amplitude

that followed the shape of the titanium screw was defined as the artifact. The pedicle screws were positioned perpendicular to the B<sub>0</sub> field. The artifact was measured along

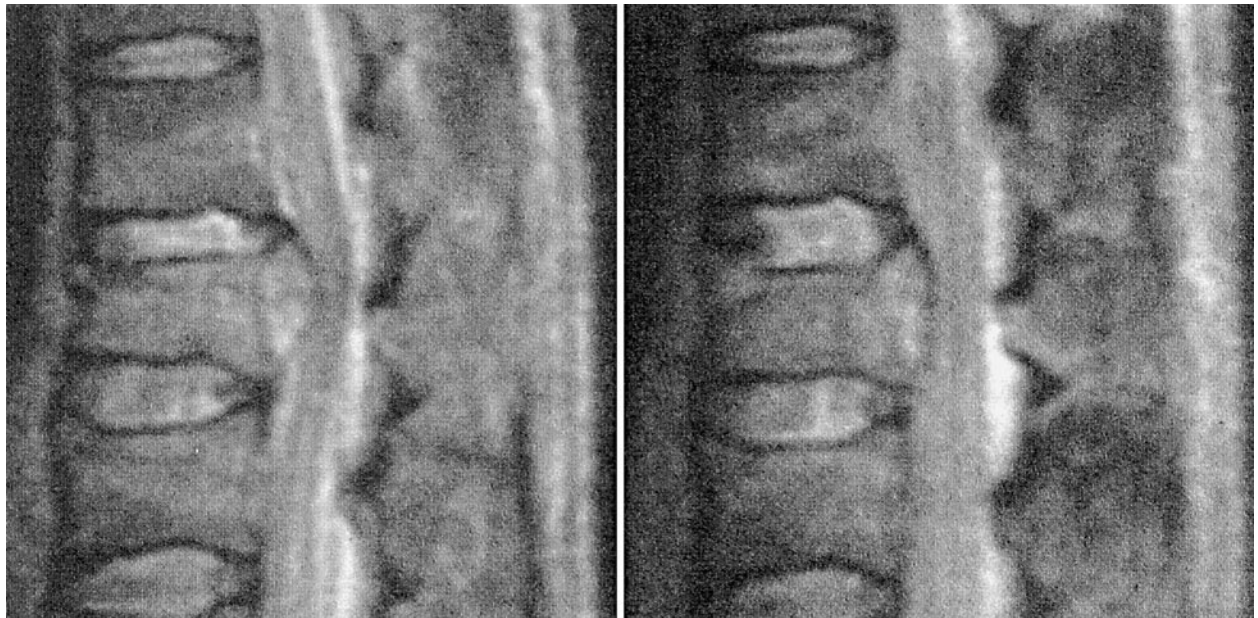


**Fig.9** Spin-echo sequences preoperative (*left*) and postoperative (*right*)

the short axis of the screw, corresponding to the frequency-encoding axis in each plane. The artifact on GE images was so severe that it was not measured. In the SE sequences, mean artifact size ranged from 231% to 364% of actual screw size. The magnification factor is bigger than in our results. However, taking into account the fact that a 1.5-T magnet was used in their study, the results do correspond to ours, because our 0.5-T magnet causes smaller artifacts. Fast spin echo sequences (FSE) caused significantly smaller artifacts than SE sequences, so did shorter TEs [16]. Muller et al. found the biggest artifact when the long axis of the implant was perpendicular to the B<sub>0</sub> field. Our results confirm that, with a maximal doubling of the artifact using SE sequences [14]. Also, Frazzini et al. found smaller artifacts when the plane of frequency encoding was parallel to the screws [6]. Lewin et al. investigated the accuracy of MR imaging for biopsy needles. They differentiated between a 0.2-T magnetic field (Magnetom Open; Siemens) and a 1.5-T magnetic field (Magnetom Vision; Siemens). In the GE sequences, the artifact was several times bigger than in the SE sequences. For SE and turbo spin echo sequences, when the frequency-encoding axis was perpendicular to the needle shaft, the apparent width of the needle was larger, but error in needle tip position was smaller. Artifacts were much less apparent, but the error in tip position increased, as the orientation of the needle shaft became more parallel to the direction of the magnetic field [12]. This corresponds with our findings, and supports the accuracy of imaging for the placement of the pedicle screws, which usually are positioned perpendicular to the B<sub>0</sub> field. So far, Ladd et al. are the only group who have

observed a shift of the artifact center away from the actual center of the needle in computer simulations. The maximum shift was 25% of the difference between the actual position of the needle and the center of the artifact. There was no shift when the long axis of the needle was parallel to the B<sub>0</sub> field, and maximum shift when the needle was perpendicular to it [9]. A clinically relevant shift was not observed in our study.

Peterman et al. saw artifacts after cervical fusions without instrumentation, and found out that particles of drill tips are responsible [15]. This was histologically proved by Heindel et al. [8]. Concerning the percutaneous insertion of an internal fixator, Wenda presented first results in 1997 [19]. We have performed this technique for selected patients since February 1997, first under fluoroscopy and now using open MRI. After two cases of aseptic seroma in the first ten patients, we changed the initially used transmuscular access to the procedure described above. Since then no further complications have been observed.

Recently developed navigation systems allow a more precise positioning of pedicle screws than conventional techniques [10]. One disadvantage of all these systems is the fact that you only can see a virtual image. The computer is working with the preoperatively acquired data. The reduction maneuver cannot be visualized, and in particular, no information can be obtained about the retropulsed posterior wall fragment. Intraoperative myelography or sonography is therefore still required. A percutaneous surgical technique supported by navigation systems has, until now, not been possible, because for "matching" (the procedure, the computer recognizes the bony structures) the dorsal surface of the vertebrae has to be exposed completely. On the other side open MRI provides us with real images with a delay of about 3 s without any matching procedure.

## Conclusion

Open MRI offers a new possibility in the therapy of unstable spine fractures. The anatomical structures of the spine can be imaged in nearly real-time. The size and configuration of the artifacts caused by instruments and implants is predictable. Exact positioning of pedicle screws can be observed intraoperatively. The most important ad-

vantage is the nearly real-time control of posterior wall fragments reduction.

Dorsal instrumentation of unstable thoracolumbar fractures with a percutaneous technique has become safe and less traumatic under MR imaging. Real-time imaging of soft tissues and bone in any plane improves safety for the patient and allows the surgeon to work less invasively and more precisely.

## References

1. Aebi M, Mohler J, Zach G, Morscher E (1986) Analysis of 75 operated thoracolumbar fractures and fracture dislocations with and without neurological deficit. *Arch Orthop Trauma Surg* 105:100–112
2. Czerovionke LF, Daniels DL, Wehrli FW, Mark LP, Hendrix LE, Strandt JA, Williams AL, Haugton VM (1988) Magnetic susceptibility artifacts in gradient-recalled echo MR imaging. *Am J Neuroradiol* 9:1149–1155
3. Degreif J, Wenda K, Ahlers J, Ritter G (1992) Experimentelle Erprobung der intraoperativen Wirbelsäulenonographie. *Unfallchirurgie* 95: 493–497
4. Degreif J, Wenda K, Runkel M, Ritter G (1994) Die Rotationsstabilität der thorakolumbalen Wirbelsäule nach interlaminärem Schallfenster, Hemilaminektomie und Laminektomie. *Unfallchirurgie* 97:250–255
5. Dick W (1987) The “Fixateur interne” as a versatile implant for spine surgery. *Spine* 9: 882–900
6. Frazzini V, Kagetsu N, Johnson C, Destian S (1997) Internally stabilized spine: optimal choice of frequency-encoding gradient direction during MR imaging minimizes susceptibility artifact from titanium vertebral body screws. *Radiology* 204:268–272
7. Fritzsche S, Thull R, Haase A (1995) Reduction of artifacts in magnetic resonance images by using optimized materials for diagnostic devices and implants. *Biomed Technik* 40:29–33
8. Heindel W, Friedman G, Bunke J, Thomas B, Firsching R, Ernestus RI (1986) Artifacts in MR imaging after surgical intervention. *J Comput Assist Tomogr* 10:596–599
9. Ladd ME, Erhart P, Debatin JF, Romanowski BJ, Boesinger P, McKinnon GC (1996) Biopsy needle susceptibility artifacts. *Magn Reson Med* 36:646–651
10. Laine T, Schlenzka D, Mäkitalo K et al (1997) Improved accuracy of pedicle screw insertion with computer-assisted surgery. *Spine* 22:1254–1258
11. Leclot H (1994) Artifacts in magnetic resonance imaging of the spine after surgery with or without implant. *Eur Spine J* 3:240–245
12. Lewin J, Duerk J, Jain V, Petersilge C, Chao C, Haaga J (1996) Needle localization in MR-guided biopsy and aspiration: effects of field strength, sequence design, and magnetic field orientation. *Am J Roentgenol* 166:1337–1345
13. Ludeke KM, Roschmann P, Tischler R (1985) Susceptibility artifacts in NMR imaging. *Magn Reson Imaging* 3:329–343
14. Mueller P, Stark D, Simeone J, Saini S, Butch R, Edelman R, Wittenberg J, Ferrucci J (1986) MR-guided aspiration biopsy needle: design and clinical trials. *Radiology* 161:605–609
15. Peterman SB, Hoffman JC, Malko JA (1991) Magnetic resonance artifact in the postoperative cervical spine. A potential pitfall. *Spine* 16:721–725
16. Petersilge C, Lewin J, Duerk J, Yoo J, Ghaneyem A (1996) Optimizing imaging parameters for MR evaluation of the spine with titanium pedicle screws. *Am J Roentgenol* 166:1213–1218
17. Rudisch A, Kremser C, Peer S, Kathrein A, Judmeier W, Daniaux H (1998) Metallic artifacts in magnetic resonance imaging of patients with spinal fusion – a comparison of implant materials and imaging sequences. *Spine* 23:692–699
18. Wang J, Yu W, Sandhu H, Tam V, Delamarter R (1998) A comparison of magnetic resonance and computed tomographic image quality after the implantation of tantalum and titanium spinal instrumentation. *Spine* 23:1684–1688
19. Wenda K, Hachenberger R, Thiem N (1997) Postoperatives MR als Entscheidungsgrundlage für rein dorsale Instrumentation oder zusätzliche ventrale Fusion bei thoracolumbalen Frakturen. *Hefte Unfallchir* 268:184–187